JOURNAL OF GUIDANCE, CONTROL, AND DYNAMICS
Vol. 21, No. 4, July–August 1998

Thermally Induced Attitude Dynamics of a Spacecraft with a Flexible Appendage

John D. Johnston* and Earl A. Thornton†
University of Virginia, Charlottesville, Virginia 22903

The performance of a significant number of spacecraft has been impacted negatively by attitude disturbances resulting from thermally induced deformations of flexible appendages. Motions of flexible appendages such as deployable booms and solar arrays result in disturbance torques reacting on the main body of a spacecraft and may have a significant effect on the attitude dynamics and control of the vehicle. The effects of thermally induced structural disturbances of a flexible appendage on the attitude dynamics of a simple spacecraft are investigated. The governing equations, including transient thermal effects, are formulated using a generalized form of Lagrange's equations for hybrid coordinate dynamical systems. An approximate solution based on modal expansion is presented for the case of a step change in solar heating that simulates an orbital eclipse transition. Analytical models are presented for the thermal–structural response of two types of flexible appendages: a thin-walled boom with tip mass and a solar panel. Numerical results demonstrate that the attitude response of the system consists of a slowly developing pointing error and superimposed oscillations whose magnitude is related to the ratio of the thermal and structural response times of the flexible appendage.

Nomenclature

A = cross-sectional area, m^2
B = Boley parameter
c = specific heat, J/kg-K
c_{damp} = damping constant, kg/m-s
E = elastic modulus, N/m^2
h = thickness, m
I = moment of inertia, m^4
I_{boom} = mass moment of inertia for flexible boom, kg-m^2
I_{hub} = mass moment of inertia for rigid hub, kg-m^2
I_{ratio} = inertia ratio
I_{sc} = composite mass moment of inertia for spacecraft, kg-m^2
I_{tip} = mass moment of inertia for tip mass, kg-m^2
k = thermal conductivity, W/m-K
L = length, m
L_{char} = characteristic length, m
M_T = thermal moment, N-m
M_{Tss} = steady-state thermal moment, N-m
m_{tip} = tip mass, kg
q = generalized modal coordinate
R = radius, m
R_{sc} = hub radius, m
S = heat flux, W/m^2
S_0 = solar heat flux, W/m^2
T = temperature, K
T_{ref} = reference temperature, K
T_{TID} = thermally induced disturbance torque, N-m
t = time, s
v = displacement, m
v_{qs} = quasistatic displacement, m
x, y, z = spatial coordinates, m
α = absorptivity
α_{cte} = coefficient of thermal expansion, 1/K
ΔT = temperature difference, K
ΔT_{ss} = steady-state temperature difference, K
ε = emissivity
ζ = damping coefficient
θ = attitude angle, rad
θ_{qs} = quasistatic attitude angle, rad
θ_{ss} = steady-state attitude angle, rad
κ = thermal diffusivity, m^2/s
ρ = density, kg/m^3
σ = Stefan–Boltzmann constant, W/m^2-K^4
τ = thermal time constant, s
ϕ = shape function
ω = natural frequency, rad/s

Received June 30, 1997; revision received Jan. 11, 1998; accepted for publication Jan. 29, 1998.

*Graduate Research Assistant, Department of Mechanical, Aerospace, and Nuclear Engineering. E-mail: jdj3y@virginia.edu. Student Member AIAA.
†Professor, Department of Mechanical, Aerospace, and Nuclear Engineering. Fellow AIAA.

Introduction

OVER the years the attitude dynamics and control of a significant number of spacecraft has been adversely affected by disturbances resulting from thermally induced structural deformations of flexible appendages.[1,2] Examples of recent spacecraft experiencing the disturbances include the Hubble Space Telescope and the Upper Atmosphere Research Satellite. Thermally induced structural disturbances are typically initiated during orbital eclipse transitions when a spacecraft exits from or enters into the Earth's shadow resulting in rapid changes in thermal loading. These sudden changes in heating may lead to the rapid development of temperature differences in structures. Temperature differences through the cross section of appendages lead to differential thermal expansion, i.e., the hot side of the appendage expands more than the cold side, which results in structural deformations. Slowly developing temperature differences lead to quasistatic deformations, whereas rapidly changing temperature differences may lead to dynamic structural motions. Motions of flexible appendages result in rigid-body rotations of the entire spacecraft, because the total angular momentum of the system is conserved. These potentially large attitude disturbances can violate mission pointing accuracy and jitter requirements. The types of flexible appendages known to experience these disturbances are: booms (gravity gradient, antennae, and scientific instrument) and solar arrays (flexible blanket and rigid panel).

Boley[3] was the first to include inertia effects in calculating the thermal–structural response of a beam subject to rapid heating and presented the governing equations for the problem of thermally induced vibrations in 1956. The approach taken by Boley was to assume that the beam deformations can be represented by the superposition of a quasistatic displacement and oscillations about that displacement. Thermally induced deformations of rigid-panel solar arrays and their effect on spacecraft control were investigated by Zimbelman.[4] He presented analyses for determining temperatures and deformations resulting from orbital eclipse transitions, but did not model the effect of solar panel dynamics (thermally induced vibrations). In recent years, a number of analytical, computational, and

experimental investigations of thermally induced vibrations have been carried out at the University of Virginia.[1,5–8] Thornton[1] includes a history of the problem and outlines approaches for obtaining several solutions. References 5–8 present recent analyses for spinning spacecraft booms and two types of flexible solar arrays. Previous analytical studies of thermally induced vibrations have considered flexible appendages fixed at their base (uncoupled dynamics) and have not considered interactions between the thermally induced dynamic motions of the appendage and the rigid-body motions of the spacecraft (coupled dynamics). This paper presents a new approach for the problem of thermally induced vibrations using a coupled dynamic formulation for a system composed of a flexible appendage attached to a rigid body. The importance of this new approach is that it gives direct insight into the effects of thermally induced vibrations on spacecraft attitude dynamics.

The objective is to investigate the effects of thermally induced structural disturbances on the attitude dynamics of a simple spacecraft consisting of a rigid hub with a cantilevered flexible appendage. The equations of motion, including transient thermal effects, are obtained using a generalized form of Lagrange's equations for hybrid coordinate dynamical systems. An approximate solution based on modal expansion is given for the case of a step change in heating, which simulates the thermal loading experienced as a spacecraft exits the Earth's shadow. Flexible appendage thermal–structural models are presented for two applications: a boom with tip mass and a solar panel. Finally, computations demonstrate the thermally induced dynamic response for the applications studied and investigate the effects of key parameters on the coupled dynamics of the system.

Mathematical Model

The problem considered is the planar motions of a simple spacecraft (Fig. 1) consisting of a rigid hub and a cantilevered flexible appendage with tip mass. The flexible appendage is modeled as a Bernoulli–Euler beam of mass per unit length ρA and bending stiffness EI. The tip mass is fixed at the free end of the appendage and has negligible rotatory inertia. Two coordinate systems used in the analysis are shown in Fig. 1. The I1–I2 axes are located in an inertial reference frame fixed with respect to motions of the spacecraft. The B1–B2 axes are located in a body-fixed reference frame attached to the hub with the B1 axis coinciding with the neutral surface of the undeformed appendage. The origins of both sets of axes coincide with the center of the hub. The attitude angle θ measures rigid-body rotations of the hub about its fixed center, and $v(x, t)$ is the displacement of the flexible appendage relative to the B1 axis. Only planar motions of the system consisting of small rotations of the hub about its center and bending vibrations of the appendage in the I1–I2 plane are considered, and there are no external forces or moments acting on the system.

Thermal–Structural Analysis

The objective of the thermal–structural analysis is to predict the transient response in terms of the temperature difference through the cross section of the appendage and the resulting thermal moment. The temperature difference is important because it induces the thermal bending of the appendage. However, the temperature distribution over the cross section of the structural member is also important because the spatial variation in temperature determines the thermal bending moment. The problem considered is a thermally induced dynamic response initiated by a sunrise orbital eclipse transition. The thermal loading consists of a uniform heat flux in the I1–I2 plane directed normal to the top surface of appendage in its undeformed state (Fig. 1). The heat flux is applied as a step function of time, such that $S = 0$ for $t < 0$ and $S = S_0$ for $t \geq 0$. It is assumed that the heat flux remains constant for small rotations of the hub and small appendage deformations, i.e., the thermal response is independent of the dynamic response. Additionally, it is assumed that the variation in the temperature along the axis of the appendage is negligible; thus, the temperature varies only through the cross section.

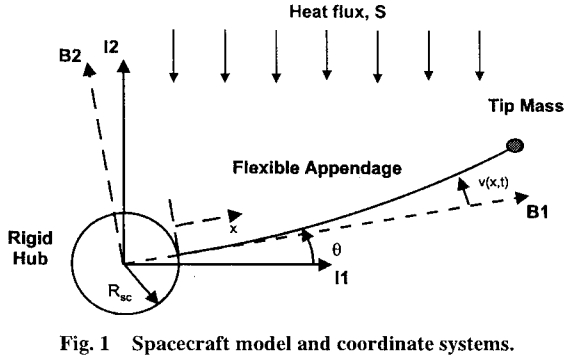

Fig. 1 Spacecraft model and coordinate systems.

Thermal response problems for spacecraft structures involve a combination of conduction and radiation heat transfer. The conservation of energy equation is nonlinear and does not lend itself to closed-form analytical solutions. The transient temperature difference for a given appendage can be determined from the governing equations and boundary conditions using finite element analysis or finite difference techniques. However, based on previous investigations[1,4] of radiantly heated spacecraft structures, the following approximate analytical expression for the transient temperature difference through the cross section of a generic appendage is proposed:

$$\Delta T(t) = \Delta T_{ss}(1 - e^{-t/\tau}) \tag{1}$$

From Eq. (1) it is seen that the temperature difference exhibits a exponential response that is typical of a first-order system subject to a step input. The thermal time constant can be estimated from the thermal diffusivity of the appendage, $\kappa = k/\rho c$, and the characteristic dimension over which the temperature varies L_{char}:

$$\tau = \frac{L_{char}^2}{\kappa} \tag{2}$$

Equation (2) provides an approximate value for the thermal time constant associated with heat transfer through the cross section of the appendage; a more accurate value can be obtained from finite element analysis. The form of the spatial variation in temperature for a particular appendage depends on the cross-sectional geometry, material properties, and the heat transfer boundary conditions. The temperature distribution $T(y, z, t) - T_{ref}$ determines the thermal bending moment

$$M_T(t) = \int_A E\alpha_{cte}[T(y, z, t) - T_{ref}]y \, dA \tag{3}$$

where $T(y, z, t)$ is the temperature through the cross section and T_{ref} is a reference temperature. Integrating Eq. (3) over the cross section of the appendage results in the following general expression for the thermal moment:

$$M_T(t) = M_{Tss}(1 - e^{-t/\tau}) \tag{4}$$

Because the temperature does not vary along the length of the appendage, the thermal moment is a function only of time. Specific results for the temperature difference and thermal moment are presented later for two applications.

Dynamics Analysis

The objective of the dynamics analysis is to predict the coupled dynamic response of the system as characterized by the attitude angle of the rigid hub, $\theta(t)$, and the displacements of the flexible appendage, $v(x, t)$. First, the equations of motion for the dynamic response of the system are formulated using an energy methods approach. Next, a solution for the quasistatic response of the system, in which inertia forces are neglected, is developed. Finally, an approximate solution for the overall dynamic response is obtained using the quasistatic solution and modal expansion.

Equations of Motion

The kinetic and potential energies, including thermal effects, for a hub-appendage type hybrid coordinate dynamical system with generalized coordinates $\theta(t)$ and $v(x, t)$ are

$$T = \frac{1}{2}I_{hub}\dot{\theta}^2 + \int_0^L \left[\frac{1}{2}\rho A\dot{v}^2 + \rho A(R_{sc} + x)\dot{\theta}\dot{v}\right] dx$$
$$+ \frac{1}{2}m_{tip}\left[\dot{v}^2(L, t) + 2(R_{sc} + L)\dot{\theta}\dot{v}(L, t)\right] \tag{5}$$

$$V = \int_0^L \left[\frac{1}{2}EI(v'')^2 + v''M_T(t)\right] dx \tag{6}$$

where T is the kinetic energy, V is the potential energy, an overdot represents differentiation with respect to time, and a prime denotes differentiation with respect to the spatial coordinate x. The kinetic energy, which neglects higher-order terms, is written in terms of the velocities of the discrete and distributed elements. The potential energy of the system includes contributions from the strain energy of the elastic appendage, including contributions from thermal strain. The thermal strain enters through the last term in Eq. (6), which includes the thermal moment given in Eqs. (3) and (4). Additionally, the nonconservative work associated with flexible appendage damping is modeled as equivalent viscous damping

$$W_{NC} = -\int_0^L c_{damp}\dot{v}\, dx \tag{7}$$

where $c_{damp} = 2\zeta\omega_n\rho A$ is the damping constant.

The equations of motion and boundary conditions for the system are formulated using a generalized form of Lagrange's equations given by Junkins and Kim.[9] The resulting governing equation for the rigid-body rotations of the spacecraft hub is

$$I_{sc}\ddot{\theta} + \int_0^L \rho A(R_{sc}+x)\ddot{v}(x,t)\, dx + m_{tip}(R_{sc}+L)\ddot{v}(L,t) = 0 \tag{8}$$

where I_{sc} is the composite mass moment of inertia for the spacecraft

$$I_{sc} = I_{hub} + \rho A\int_0^L (R_{sc}+x)^2\, dx + m_{tip}(R_{sc}+L)^2 \tag{9}$$

An expression for the thermally induced disturbance torque can be obtained from Eq. (8) by moving the terms corresponding to motions of the flexible appendage to the right-hand side of the equation:

$$T_{TID}(t) = -\left[\int_0^L \rho A(R_{sc}+x)\ddot{v}(x,t)\, dx + m_{tip}(R_{sc}+L)\ddot{v}(L,t)\right] \tag{10}$$

The governing equation for the appendage deformations in the body-fixed reference frame is given by

$$\rho A(R_{sc}+x)\ddot{\theta} + \rho A\ddot{v} + c_{damp}\dot{v} + EIv^{IV} = 0 \tag{11}$$

At $x = 0$, the appendage is cantilevered, and the geometric boundary conditions are

$$v(0,t) = 0 \tag{12a}$$

$$v'(0,t) = 0 \tag{12b}$$

At $x = L$, the appendage supports the tip mass and the natural boundary conditions for shear force and bending moment are

$$EIv'''(L,t) = m_{tip}[\ddot{v}(L,t) + (R_{sc}+L)\ddot{\theta}] \tag{12c}$$

$$EIv''(L,t) + M_T(t) = 0 \tag{12d}$$

Equation (12c) represents the shear force on the tip mass, and Eq. (12d) represents the moment acting on the tip mass, where the right-hand side is zero because the rotatory inertia of the tip mass is neglected.

Quasistatic Response

A quasistatic response occurs for the case where inertia effects are negligible, i.e., there are no dynamical effects (oscillations). The quasistatic structural response consists of a succession of equilibrium displacements each corresponding to the temperature distribution at a given instant in time. The quasistatic displacements are obtained by neglecting terms corresponding to inertia forces in Eqs. (11) and (12)

$$EIv_{qs}^{IV} = 0 \tag{13a}$$

$$v_{qs}(0,t) = 0, \qquad v'_{qs}(0,t) = 0$$
$$v''_{qs}(L,t) = \frac{-M_T(t)}{EI}, \qquad v'''_{qs}(L,t) = 0 \tag{13b}$$

Solving Eq. (13a) subject to the boundary conditions, Eq. (13b), yields the solution for the quasistatic displacements of the appendage:

$$v_{qs}(x,t) = \frac{-M_T(t)}{2EI}x^2 \tag{14}$$

The quasistatic attitude angle is obtained by setting $v(x,t) = v_{qs}(x,t)$ in Eq. (8), which gives

$$\theta_{qs}(t) = \theta_{ss}(1 - e^{-t/\tau}) \tag{15}$$

where the steady-state quasistatic attitude angle is given by

$$\theta_{ss} = \frac{M_{Tss}}{2EII_{sc}}\left[\rho A\left(\frac{R_{sc}L^3}{3} + \frac{L^4}{4}\right) + m_{tip}\left(R_{sc}L^2 + L^3\right)\right] \tag{16}$$

Physically, the quasistatic attitude angle corresponds to the pointing error induced through the action of the thermally induced quasistatic deformation of the flexible appendage. The steady-state quasistatic attitude angle is then a measure of the steady-state pointing error induced by the appendage deformations. Later, it will be seen that oscillations about the quasistatic attitude response (so-called jitter) will result from appendage vibrations.

Approximate Transient Solution

An approximate form of the equations of motion stated in Eqs. (8) and (11) is obtained using the quasistatic solution and a modal expansion. The assumed form of the solution is

$$v(x,t) = v_{qs}(x,t) + \sum_{n=1}^{N} q_n(t)\phi_n(x) \tag{17}$$

where $q_n(t)$ are the nth generalized modal coordinates, $\phi_n(x)$ are the nth shape functions, and N is the number of modes. The shape functions are chosen to be the eigenfunctions from the free vibration response of a fixed-base cantilevered beam with tip mass. The approximate equations of motion for the system are obtained by substituting the assumed form of the solution into Eqs. (8) and (11). Substituting first into Eq. (8) and rearranging gives

$$I_{sc}\ddot{\theta} + \sum_{n=1}^{N}\left[\rho A\int_0^L (R_{sc}+x)\phi_n\, dx + m_{tip}(R_{sc}+L)\phi_n(L)\right]\ddot{q}_n$$
$$= -\rho A\int_0^L (R_{sc}+x)\ddot{v}_{qs}\, dx - m_{tip}(R_{sc}+L)\ddot{v}_{qs}(L,t) \tag{18}$$

Next, Eq. (11) is multiplied by $\phi_m(x)$, and integrated over $0 \le x \le L$. Substituting in Eq. (17) and using integration by parts twice to introduce the boundary conditions at $x = L$ yields

$$\left[\rho A\int_0^L (R_{sc}+x)\phi_m\, dx + m_{tip}(R_{sc}+L)\phi_m(L)\right]\ddot{\theta}$$
$$+ \sum_{n=1}^{N}\left[\rho A\int_0^L \phi_n\phi_m\, dx + m_{tip}\phi_n(L)\phi_m(L)\right]\ddot{q}_n$$
$$+ \sum_{n=1}^{N}\left[c_{damp}\int_0^L \phi_n\phi_m\, dx\right]\dot{q}_n + \sum_{n=1}^{N}\left[EI\int_0^L \phi''_n\phi''_m\, dx\right]q_n$$
$$= -\left\{\int_0^L [\rho A\ddot{v}_{qs} + c_{damp}\dot{v}_{qs}]\phi_m\, dx + m_{tip}\ddot{v}_{qs}(L,t)\phi_m(L)\right\} \tag{19}$$

where $m = 1, 2, \ldots, N$. Thus, the governing equations have been reduced to a set of $N + 1$ coupled linear ordinary differential equations for the discrete coordinate $\theta(t)$ and the generalized modal coordinates $q_n(t)$. These equations can be written in matrix form as

$$[M]\{\ddot{X}\} + [C]\{\dot{X}\} + [K]\{X\} = \{F(t)\} \tag{20}$$

where $\{X\}^T = \{\theta \ q_1 \ q_2 \ \cdots \ q_N\}$ are the generalized coordinates for the system, and $[M]$, $[C]$, and $[K]$ are $N + 1$ by $N + 1$ constant coefficient matrices. The mass matrix is symmetric and includes off-diagonal terms, which express coupling between the discrete and distributed generalized coordinates. The stiffness and damping matrices are both symmetric and diagonal. Numerical integration of Eq. (20) leads to solutions for the thermally induced attitude dynamics of the system.

Characteristic Parameters

It is possible to gain some insight into the character of the thermal–structural response of a flexible appendage prior to undertaking a detailed numerical study. A key parameter for assessing the potential of a thermally induced dynamic response is given by Boley and Weiner.[10] The Boley parameter is defined as the square root of the ratio of the characteristic thermal and structural response times of the system:

$$B = \sqrt{t_T/t_s} \tag{21}$$

where the characteristic thermal response time t_T is given by Eq. (2) and the characteristic structural response time t_s is the period of the fundamental mode of vibration for the appendage. Boley also developed a relation for the dynamic amplification factor that gives the ratio of the maximum dynamic displacement to the maximum quasistatic displacement:

$$\frac{v_{\text{dynamic}}}{v_{\text{static}}} = 1 + \frac{1}{\sqrt{1 + B^2}} \tag{22}$$

From Eq. (22) it can be seen that for large values of B the dynamic amplification factor is on the order of one. Under these circumstances quasistatic thermal–structural analysis is justified. This is the case for a majority of terrestrial structures. For small values of B the dynamic amplification factor is greater than one, and inertial terms should be included in the thermal–structural analysis. Structures with a value of B on the order of one are typically susceptible to thermally induced vibrations when subjected to rapid heating.

Applications

A numerical study was performed to investigate the attitude dynamics of the system resulting from thermally induced vibrations of two types of flexible appendages: a boom with tip mass and a solar panel. Results were obtained by performing numerical integration of the equations of motion using the central difference method. The simulations utilized $N = 5$ flexible modes, with a timestep based on the highest mode included. The simple spacecraft used in the study has a rigid hub with a mass moment of inertia of 1250 kg-m^2 and a radius of 1.0 m. Table 1 presents a list of properties for the flexible appendages.

Table 1 Flexible appendage properties

Property	Boom	Solar panel
ρA, kg/m	0.087	1.77
EI, N-m^2	84	817
α_{cte}, 1/K	1.69E-05	2.3E-05
ζ	0.001	0.001
ρ, kg/m^3	8026	36.8 (honeycomb core)
k, W/m-K	16.6	1.5 (honeycomb core)
c, J/kg-K	502	921 (honeycomb core)
α	0.30	0.79 (upper)
ε	0.13	0.81 (upper), 0.86 (lower)

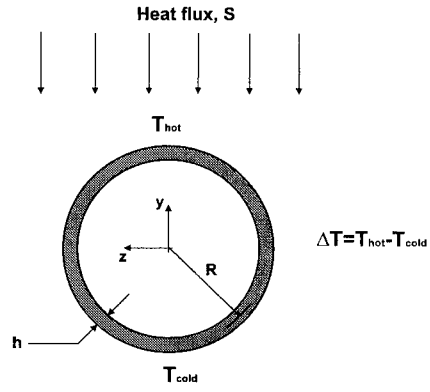

Fig. 2 Spacecraft boom cross-sectional geometry.

Boom with Tip Mass

The first application studied is a boom with tip mass.[11] This application is useful for studying the behavior of deployable booms that support a scientific instrument or other payloads at their free end. The boom (Fig. 2) is modeled as a thin-walled circular cross-sectional tube of radius R and wall thickness h. The thermal model assumes one-dimensional conduction around the circumference of the tube and heat loss from emitted radiation on its external surface. An approximate analytical solution for the temperature distribution is given by Thornton.[1] The magnitude of the temperature difference has the form

$$\Delta T(t) = (\alpha S_0 \tau/\rho c h)(1 - e^{-t/\tau_{\text{tube}}}) \tag{23}$$

where

$$\tau_{\text{tube}} = \left[(k/\rho c R^2) + (4\sigma\varepsilon/\rho c h) \cdot (\alpha S_0/\pi\sigma\varepsilon)^{\frac{3}{4}}\right]^{-1} \tag{24}$$

is the thermal time constant. The form of Eq. (24) is similar to the form of the thermal time constant proposed in Eq. (2). The first term in Eq. (24) is associated with conduction heat transfer and the second term corresponds to radiation heat transfer. For typical metallic spacecraft booms the first term dominates the thermal time constant justifying the form of Eq. (2). The thermal moment is obtained by integrating Eq. (3) over the cross section of the boom

$$M_T(t) = \tfrac{1}{2}\pi E \alpha_{\text{cte}} h R^2 \Delta T_{\text{ss}}(1 - e^{-t/\tau_{\text{tube}}}) \tag{25}$$

The model utilized in the numerical study uses properties for a stainless-steel Bi-STEM boom with a length of 7.5 m, a radius of 9.53E-03 m, a wall thickness of 2.03E-04 m, and a 1.5-kg tip mass. The thermal time constant is 22.02 s from Eq. (2) and 21.93 s from Eq. (24). The boom has a fixed-base (constrained) fundamental frequency of 0.096 Hz, which, using Eq. (2) for t_T, results in a value of 1.45 for the Boley parameter. For this value of B we may expect thermally induced oscillations. Figure 3 presents the transient temperature difference through the cross section of the boom due to the suddenly applied heat flux. The temperature difference reaches a steady-state value of 11 K in approximately 150 s. The corresponding boom deformations are shown in Fig. 4, which presents the tip displacement in the body-fixed reference frame. The motions consist of a quasistatic displacement and superimposed oscillations. The quasistatic displacement has a steady-state value of −0.34 m. The oscillations have a peak to peak magnitude of 0.05 m and occur at a frequency of 0.10 Hz, which corresponds to the fundamental mode for the combined (unconstrained) rigid-hub/boom system. Because of the conservation of angular momentum, the hub undergoes rotations in the direction opposite to the boom motions. The attitude angle response (Fig. 5) consists of a slowly developing quasistatic rotation (pointing error) and superimposed oscillations (jitter). The pointing error has a steady-state value of 0.20 deg and the jitter has a 0.03-deg peak-to-peak amplitude. The rigid-body rotations occur at the same frequency as the flexible boom vibrations.

A parameter study was completed to investigate the effects of varying the rigid-hub mass moment of inertia on the dynamic response of the system. The study utilized the same boom and

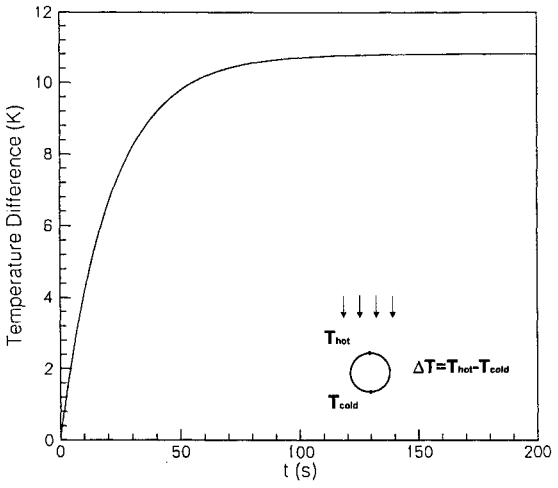

Fig. 3 Temperature difference vs time for boom with tip mass.

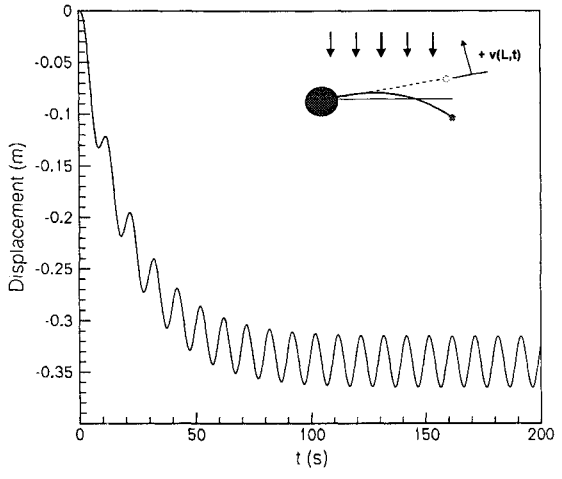

Fig. 4 Tip displacement vs time for boom with tip mass.

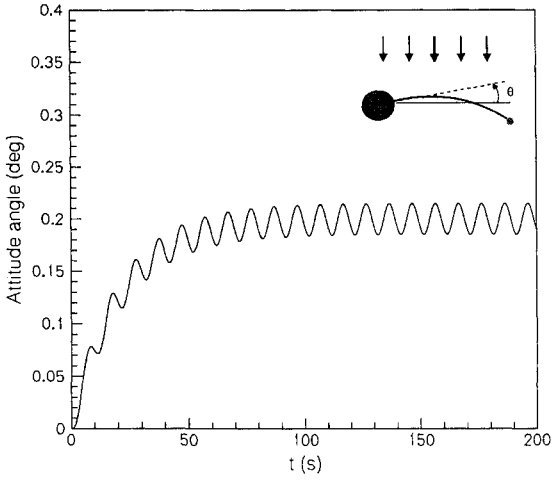

Fig. 5 Attitude angle vs time for boom with tip mass.

tip mass parameters as in the preceding section. The hub radius was maintained at 1.0 m, and I_{hub} was varied between 125 and 12,500 kg-m^2. The results of the study are presented in Fig. 6 in terms of a dimensionless inertia ratio, $I_{ratio} = I_{hub}/(I_{boom} + I_{tip})$. The following trends are observed as the inertia ratio increases: 1) the frequency of the disturbance approaches the fundamental frequency of a fixed-base cantilever beam (0.96 Hz), 2) the magnitude of the steady-state attitude angle (pointing error) approaches zero, and 3) the peak amplitude of the attitude oscillations (jitter) approaches zero. Thermally induced structural disturbances occur at the fundamental frequency of the combined rigid-hub/flexible-

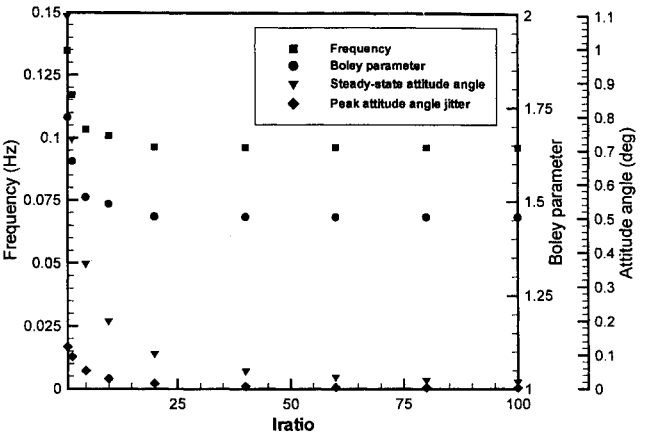

Fig. 6 Dynamic response as a function of inertia ratio.

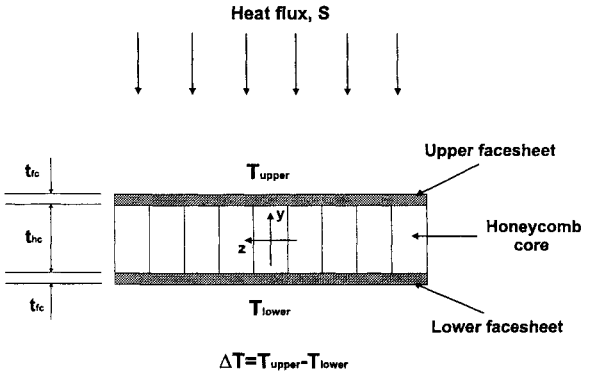

Fig. 7 Solar panel cross-sectional geometry.

appendage system. As the mass moment of inertia of the rigid hub increases, the fundamental frequency of the system and the corresponding disturbances decrease to the frequency of a fixed-base cantilever beam, which is in agreement with previous research[12] that has shown that unconstrained natural frequencies approach constrained (fixed-base) natural frequencies from above as rigid-body inertia increases.

Note that the coupled dynamic formulation correctly predicts the change in the disturbance frequency with changing inertia ratio, whereas a fixed-base thermally induced vibrations formulation only gives the correct frequency for systems with large values of I_{ratio}. In terms of the attitude response, as the mass of the hub becomes large the rigid-body inertia of the system approaches infinity, and the torque resulting from motions of the boom and tip mass has a diminishing influence. Conversely, as the inertia ratio approaches unity, the pointing error and jitter dramatically increase, which has important implications for small satellite design.

Solar Panel

The second application represents the behavior of solar panels[13] that utilize a honeycomb sandwich construction. The panel cross-sectional geometry (Fig. 7) consists of a honeycomb core onto which are bonded upper and lower facesheets. The honeycomb core is modeled as a uniform solid using effective properties based on the core cell size and foil gauge. The effects of solar cells, coverglass, and adhesives are neglected. The thermal model assumes one-dimensional conduction through the thickness of the panel and emitted radiation on the upper and lower surfaces. The temperature of the solar array, $T(y, t)$, is assumed to be independent of x and z and to vary only through the thickness of the array in the y direction. The temperature is assumed constant through the thickness of the facesheets, where $T_{upper}(t)$ and $T_{lower}(t)$ are the temperatures of the upper and lower facesheets, respectively. Thus, the temperature varies only through the honeycomb core, and the temperature difference through the thickness is given by $\Delta T(t) = T_{upper}(t) - T_{lower}(t)$. The steady-state temperature difference can be obtained by writing the heat balance equations at thermal equilibrium.[14] At steady state, the heat

absorbed is balanced by the heat radiated from the upper and lower surfaces by thermal radiation:

$$\alpha_{\text{upper}} S_0 = \sigma \varepsilon_{\text{upper}} T_{\text{upper}}^4 + \sigma \varepsilon_{\text{lower}} T_{\text{lower}}^4 \tag{26}$$

Additionally, at steady state the heat flux through the thickness of the honeycomb core is balanced by the thermal radiation flux from the lower surface:

$$k_{\text{hc}} \frac{(T_{\text{upper}} - T_{\text{lower}})}{t_{\text{hc}}} = \sigma \varepsilon_{\text{lower}} T_{\text{lower}}^4 \tag{27}$$

Equations (26) and (27) can be solved using an iterative solution technique to obtain the upper and lower surface temperatures and the corresponding steady-state temperature difference. The thermal time constant is found from Eq. (2) using the thermal diffusivity of the honeycomb core and the characteristic dimension over which the temperature varies, in this case, the thickness of the honeycomb core. Comparison with finite element analyses shows that iteratively solving Eqs. (26) and (27) gives the correct value for the steady-state temperature difference. The value for the thermal time constant from Eq. (2) is 20% greater than the value obtained from finite element analysis because the approximate expression neglects contributions from radiation heat transfer. Thus, finite element analysis provides a more accurate determination of the thermal time constant for solar panels. The thermal moment for the panel is obtained from Eq. (3) by assuming that only the facesheets contribute to the bending stiffness of the solar panel:

$$M_T(t) = \frac{E I \alpha_{\text{ctc}} \Delta T_{\text{ss}}}{h} (1 - e^{-t/\tau_{\text{panel}}}) \tag{28}$$

where h is the distance between the centroids of the upper and lower facesheets.

The solar panel studied consists of 2.54E-04-m-thick aluminum (6061-T6 alloy) facesheets and an 9.525E-03-m-thick aluminum (5056 alloy) honeycomb core with a cell size of 6.35E-03 m and a nominal foil gauge of 2.54E-05 m. The solar panel has a length of 7.5 m and a width of 1.0 m. The thermal time constant, from Eq. (2), is $t_T = 1.99$ s and the panel has a fixed-base fundamental frequency of 0.21 Hz, which results in a Boley parameter of 0.65. For B in this range, we again expect thermally induced oscillations. Figure 8 presents the transient temperature difference through the thickness of the solar panel from Eq. (1). The temperature difference reaches a steady-state value of 3.3 K in approximately 10 s. Figure 9 presents a plot of the solar panel displacements at the free end ($x = L$) in the body-fixed reference frame. The motions consist of a quasistatic displacement and superimposed oscillations. The quasistatic displacement has a steady-state value of −0.22 m. The oscillations, which are seen to decay due to damping, have a maximum peak-to-peak amplitude of 0.12 m and occur at a frequency of 0.24 Hz. The attitude response (Fig. 10) consists of a slowly developing pointing error superimposed with decaying oscillations. The

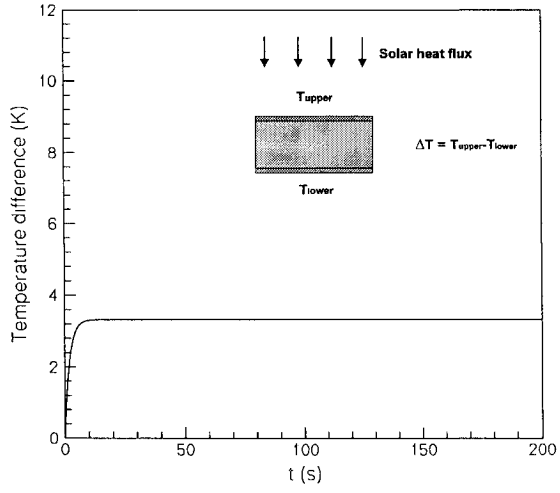

Fig. 8 Temperature difference vs time for solar panel.

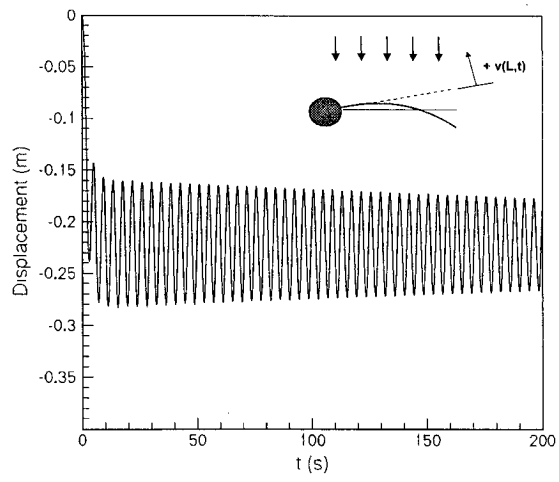

Fig. 9 Tip displacement vs time for solar panel.

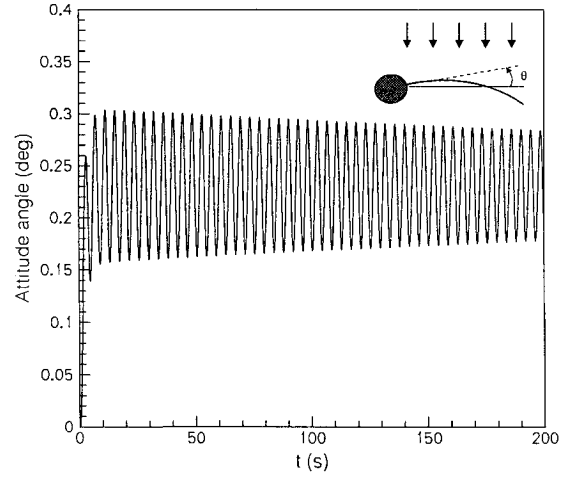

Fig. 10 Attitude angle vs time for solar panel.

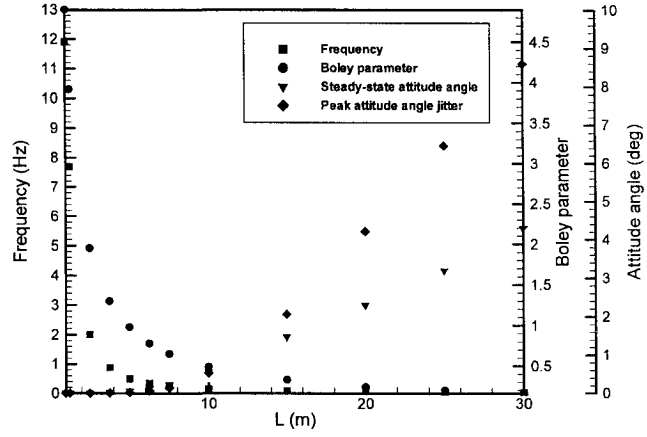

Fig. 11 Dynamic response as a function of solar panel length.

pointing error has a steady-state value of 0.23 deg, and the decaying oscillations have a 0.15-deg maximum peak-to-peak amplitude (jitter).

A parameter study using the same rigid hub and solar panel properties as the preceding example investigated the effect of varying solar panel length between 1.0 and 30.0 m on the dynamic response of the system. The following trends are observed in Fig. 11 as the length of the solar panel increases: 1) the frequency of the thermally induced structural disturbance decreases, 2) the magnitude of the steady-state attitude angle (pointing error) increases, and 3) the amplitude of the attitude angle oscillations (jitter) increases. The total mass of the solar panel increases with increasing length,

which results in a decrease in the frequency of rigid-hub/solar panel system and the corresponding thermally induced structural disturbance. The increase in pointing error is also due to the increase in solar panel mass, which leads to an increase in the magnitude of the disturbance torque reacting on the hub. The decrease in the fundamental frequency of the system leads to a corresponding decrease in the Boley parameter. Recall that as the Boley parameter decreases, the dynamic amplification factor increases, i.e., there is an increase in the ratio of the maximum dynamic displacement to the maximum quasistatic displacement for the solar panel. This results in a corresponding increase in the ratio of the maximum attitude angle to the quasistatic attitude angle. Thus, the attitude dynamics of the system are related to the Boley parameter B, where for large values of B the attitude response consists of a slowly developing pointing error (quasistatic response) and for small values the response consists of a pointing error and superimposed jitter, where the ratio of the peak dynamic attitude angle to the peak quasistatic attitude angle approaches a maximum of 2.0 as $B \rightarrow 0$.

Conclusions

A formulation for studying the attitude dynamics of a simple spacecraft incorporating the effects of a flexible appendage undergoing thermally induced vibrations has been presented. The governing equations, including transient thermal effects, were developed using a generalized form of Lagrange's equations for hybrid coordinate dynamical systems. The formulation was then utilized to study the problem of the dynamic response to a step change in solar heating for two types of flexible appendages: a thin-walled boom with tip mass and a solar panel. Results from the numerical study showed that 1) the dynamic response of the flexible appendage consists of a quasistatic displacement and superimposed oscillations whose magnitude is related to the Boley parameter $B = \sqrt{(t_T/t_s)}$, where t_T is the thermal time constant and t_s is the period of the fundamental mode of vibration; 2) due to conservation of angular momentum the hub undergoes rigid-body rotations in the direction opposite to the appendage deformations; 3) the dynamic response of the system is at the frequency of the fundamental mode of the combined rigid-hub/flexible-appendage system; and 4) systems for which $B \gg 1.0$ will undergo a quasistatic response, and those for which $B \approx 1.0$ will experience a thermally induced dynamic response. In conclusion, the coupled dynamic formulation for thermally induced attitude dynamics presented offers several advantages over previous fixed-base thermally induced vibrations (uncoupled dynamics) formulations, because the new formulation predicts the thermally induced dynamics of both the spacecraft and the appendage and also correctly predicts the frequency of the disturbance for a range of spacecraft inertia ratios.

Acknowledgments

This research is funded by the NASA Graduate Student Researchers Program. The authors appreciate the support of our technical advisors Brantley Hanks and Marvin Rhodes of NASA Langley Research Center.

References

[1]Thornton, E. A., *Thermal Structures for Aerospace Applications*, AIAA Education Series, AIAA, Reston, VA, 1996, Chap. 9.

[2]Johnston, J. D., and Thornton, E. A., "An Evaluation of Thermally-Induced Structural Disturbances of Spacecraft Solar Array Structures," *Proceedings of the 31st Intersociety Energy Conversion Engineering Conference*, Inst. of Electrical and Electronics Engineers, Washington, DC, 1996, pp. 1–6; also Paper 96-080, Aug. 1996.

[3]Boley, B. A., "Thermally Induced Vibrations of Beams," *Journal of the Aeronautical Sciences*, Vol. 23, No. 2, 1956, pp. 179–181.

[4]Zimbelman, D. F., "Thermal Shock and Its Effect on Spacecraft Attitude Control," Ph.D. Dissertation, Dept. of Aerospace Engineering Sciences, Univ. of Colorado, Boulder, CO, Aug. 1990.

[5]Johnston, J. D., and Thornton, E. A., "Thermal Response of Radiantly Heated Spinning Spacecraft Booms," *Journal of Thermophysics and Heat Transfer*, Vol. 10, No. 1, 1996, pp. 60–68.

[6]Gulick, D., and Thornton, E. A., "Thermally Induced Vibrations of an Axial Boom on a Spin-Stabilized Spacecraft," *Acta Astronautica*, Vol. 36, No. 3, 1995, pp. 163–176.

[7]Thornton, E. A., and Kim, Y. A., "Thermally Induced Bending Vibrations of a Flexible Rolled-Up Solar Array," *Journal of Spacecraft and Rockets*, Vol. 30, No. 4, 1993, pp. 438–448.

[8]Thornton, E. A., Chini, G. P., and Gulick, D. W., "Thermally-Induced Vibrations of a Self-Shadowed Split Blanket Solar Array," *Journal of Spacecraft and Rockets*, Vol. 32, No. 2, 1995, pp. 302–311.

[9]Junkins, J. L., and Kim, Y., *Introduction to Dynamics and Control of Flexible Structures*, AIAA Education Series, AIAA, Washington, DC, 1993, pp. 148–156.

[10]Boley, B. A., and Weiner, J. H., *Theory of Thermal Stresses*, Wiley, New York, 1960, pp. 339–345.

[11]Johnston, J. D., and Thornton, E. A., "Thermally-Induced Attitude Dynamics of a Spacecraft with a Flexible Boom," American Astronautical Society/AIAA Spaceflight Mechanics Symposium, AAS Paper 97-178, Huntsville, AL, Feb. 1997.

[12]Hughes, P. C., "Attitude Dynamics of a Three-Axis Stabilized Satellite with a Large Flexible Solar Array," AIAA Paper 72-857, Aug. 1972.

[13]Johnston, J. D., and Thornton, E. A., "Thermally-Induced Structural Disturbances of Rigid Panel Solar Arrays," *Proceedings of the 1997 Flight Mechanics Symposium*, NASA CP 3345, 1997, pp. 33–47.

[14]Bainum, P. M., Hamsath, N., and Krishna, R., "The Dynamics and Control of Large Space Structures After the Onset of Thermal Shock," *Acta Astronautica*, Vol. 19, No. 1, 1980, pp. 1–8.